have been attempted in the event that only the X-band downlink, coherent with the S-band uplink, were available. In this case the IPT signature would be imposed on the S-band uplink and then transponded to ground at the standard DSN frequency turnaround ratio of 880/221. If we compare the X-band received frequency with an orbit-corrected frequency prediction, it is still technically possible to extract the subtle phase shift expected from the IPT. For all practical purposes, however, the Doppler shifts expected from the gravitational perturbations of the Jovian moons and higher moments of Jupiter's gravity field would all tend to mask the desired signal.

13. M. K. Bird and P. Edenhofer, in *Physics of the Inner Heliosphere*, R. Schwenn and E. Marsch, Eds. (Springer-Verlag, Heidelberg, 1990), vol. 1, chap. 2; M. K. Bird, *Space Sci. Rev.* **33**, 99 (1982).
14. G. L. Tyler, *Proc. IEEE* **75**, 1404 (1987).
15. N. Divine and H. B. Garrett, *J. Geophys. Res.* **88**, 6889 (1983).
16. It can be shown that the differential frequency residual will have a small bias due to the spin of the spacecraft. For the Ulysses S/X-band system, the bias from the nominal 5-rpm spacecraft rotation f_{spin} will amount to $f_{bias} = 8f_{spin}/11$. The attitude control data during the IPT occultation indicate that the actual spin period was 12.039 s, so that $f_{bias} \simeq 0.0604$ Hz.
17. R. G. Stone *et al.*, *Science*, **257**, 1524 (1992).
18. A. J. Dessler and T. W. Hill, *Geophys. Res. Lett.* **2**, 567 (1975).
19. L. Trafton, *Icarus* **42**, 111 (1980); J. T. Trauger, G. Münch, F. L. Roesler, *Astrophys. J.* **236**, 1035 (1980); C. B. Pilcher and J. S. Morgan, *ibid.* **238**, 375 (1980). A recent review of optical observations of the IPT and its associated neutral clouds has been written by N. Thomas, *Surv. Geophys.*, in press.
20. As described by H. T. Howard *et al.* [*Space Sci. Rev.* **60**, 565 (1992)], the geometrical constellations assumed by the Galileo spacecraft during its Jupiter tour beginning in late 1995 will provide many opportunities to repeat this occultation experiment. The harsh radiation environment of the IPT will restrict in situ investigation of the IPT with Galileo to the inbound and outbound passes surrounding the Jupiter orbit insertion. Unfortunately, Galileo will be severely handicapped in its radio science program at Jupiter unless that spacecraft's problematic high gain antenna (HGA) is successfully deployed. Should the HGA remain nonfunctional, the only available downlink will be at S-band from either of two low gain antennas (LGAs). In addition to a loss of some 30 dB going from the HGA to the LGA, it will be very difficult to isolate the effects of plasma variations along the signal's propagation path without exploiting the dispersive Doppler shift from the originally designed phase-coherent downlinks at both S- and X-band.
21. The IPT occultation experiment could not have been performed without the outstanding efforts of the Radio Science Support Team at the Jet Propulsion Laboratory. We acknowledge especially valuable contributions from A. S. Devereaux, P. M. Eshe, R. G. Herrera, T. Horton, and D. D. Morabito. We thank F. Bagenal for supplying us with a hand-tailored IPT model that could be most effectively used in our simulation studies. We appreciate the encouragement for the IPT occultation experiment and the many helpful comments to this initial report provided by A. J. Dessler. Much of the research described in this paper was carried out at the Jet Propulsion Laboratory, California Institute of Technology, under a contract with the National Aeronautics and Space Administration. This paper presents results of a research project partially funded by the Deutsche Agentur für Raumfahrtangelegenheiten GmbH under contract 50 ON 9104, and by the Deutsche Forschungsanstalt für Luft- und Raumfahrt, Institut für Hochfrequenztechnik, NE-HF. The responsibility for the contents of this publication is assumed by the authors.

1 June 1992; accepted 11 August 1992

Plasma Composition in Jupiter's Magnetosphere: Initial Results from the Solar Wind Ion Composition Spectrometer

J. Geiss, G. Gloeckler, H. Balsiger, L. A. Fisk, A. B. Galvin, F. Gliem, D. C. Hamilton, F. M. Ipavich, S. Livi, U. Mall, K. W. Ogilvie, R. von Steiger, B. Wilken

The ion composition in the Jovian environment was investigated with the Solar Wind Ion Composition Spectrometer on board Ulysses. A hot tenuous plasma was observed throughout the outer and middle magnetosphere. In some regions two thermally different components were identified. Oxygen and sulfur ions with several different charge states, from the volcanic satellite Io, make the largest contribution to the mass density of the hot plasma, even at high latitude. Solar wind particles were observed in all regions investigated. Ions from Jupiter's ionosphere were abundant in the middle magnetosphere, particularly in the high-latitude region on the dusk side, which was traversed for the first time.

The interaction of the solar wind with planets, the moon, or comets takes on different forms, and comparative studies of these interactions are an important part of space plasma physics and solar system research. For example, the main energy for magnetospheric processes is believed to be supplied by the solar wind in the case of Earth but by the planet's rotation in the case of Jupiter (*1*, *2*). In fact, the Jovian magnetosphere is characterized by significant plasma pressures and strong centrifugal forces resulting from the fast rotation of the planet, its strong magnetic field, and a large abundance of heavy ions from the volcanic satellite Io. With the Solar Wind Ion Composition Spectrometer (SWICS) on board Ulysses, we obtained representative and comprehensive data on the plasma composition in the Jovian magnetosphere, allowing us to study sources and transport of different ion species. This information also enables us to determine the mass loading in the rotating magnetic field of Jupiter, which in turn determines the effect of centrifugal forces on the overall geometry and dynamics of the Jovian magnetosphere. In this report we give a preliminary account of our findings.

The design of SWICS, its capabilities, operational modes, and performance in flight are described in (*3*). The instrument combines energy-per-charge separation by an electrostatic analyzer (0.6 to 60 keV/*e*), acceleration (23 kV), time-of-flight measurement, and determination of total energy with solid-state detectors. For an ion producing a triple coincidence (two time-of-flight and one solid-state detector signals), this technique allows the determination of its mass (M) and charge (q) separately so that different ion species can be distinguished even if they have equal M/q ratios. A double coincidence (time-of-flight only) permits only measurement of the M/q ratio (*4*). The coincidence methods used suppress background, an important feature in the strong radiation fields of the Jovian magnetosphere (*5*).

SWICS is optimized for solar wind conditions. The collimator accepts ions arriving in a cone of 60° half-width around the spin axis pointing toward Earth. Thus, SWICS covered only a part of the angular distribution of the magnetospheric ions. In particular, it viewed the corotation direction only on the outbound, dusk, high-latitude path.

Figure 1 gives an overview of the ion populations from 0.6 to 60 keV/*e* we encountered in the Jovian environment. The bow-shock crossings are readily recognizable in the SWICS data: the count rates for H^+ and He^{2+} were reduced in the magnetosheath because there, in the high-temperature, low-speed environment, our instrument did not cover the whole energy range and angular distribution of these ions as it does in the highly supersonic solar wind. The multiple entries into and exits out of the magnetosphere were marked by the prompt appearance and disappearance of S and low-charge O ions, as well as by increased background counts caused by penetrating electrons in the individual detectors. For instance, the short excursion back into the magnetosheath (actually, a mixed

J. Geiss, H. Balsiger, U. Mall, R. von Steiger, Physikalisches Institut, Universität Bern, 3012 Bern, Switzerland.
G. Gloeckler, A. B. Galvin, D. C. Hamilton, F. M. Ipavich, Department of Physics, University of Maryland, College Park, MD 20742.
L. A. Fisk, Office of Space Science and Applications, National Aeronautics and Space Administration, Washington, DC 20546.
F. Gliem, Institut für Datenverarbeitende Anlagen, Technische Universitat, 3300 Braunschweig, Germany.
S. Livi and B. Wilken, Max-Planck-Institut fur Aeronomie, 3411 Katlenburg-Lindau, Germany.
K. W. Ogilvie, National Aeronautics and Space Administration, Goddard Space Flight Center, Greenbelt, MD 20770.

plasma region) on the inbound path between ~96 and ~87 Jovian radii (R_J) was marked by a decrease in Iogenic ions and an increase in solar wind H^+ and He^{2+}. Iogenic S and O ions were abundant everywhere in the magnetosphere, even during the period when Ulysses reentered the magnetosphere on the outbound pass at high southern latitude at a distance from Jupiter as large as 115 to 125 R_J (6).

From general plasma characteristics (Fig. 1), we determined when Ulysses was inside the magnetosphere proper (excluding the mixed plasma regions) and chose for our initial analysis seven pure magnetospheric regions along Ulysses' path (Table 1). Data on the angles between the magnetic field (7) (*B* field) and spin axis are included in Table 1, to indicate our ability to see field-aligned ion streams. In Fig. 2 the ion population in the magnetosphere is compared with a typical solar wind ion population. Triple coincidence pulse height events are presented in an M versus M/*q* scatter plot, and double coincidences are shown below in an M/*q* spectrum. Whereas a considerable fraction of ions with two or more charges produced triple coincidences, singly charged ions registered mainly as double coincidences. Thus, O^+ and especially S^+ were rare in the M versus M/*q* plot. H^+ and He^{2+} were also suppressed by our priority scheme. With calibration data, the detection efficiencies for triple and double coincidences as well as the differences in priority can be corrected to obtain ion abundance ratios. Figure 2 shows the excellent M/*q* separation of the instrument and the degree of mass separation between S and O ions. Although there was some overlap between O^{2+} and S^{4+} and between O^+ and S^{2+}, the amount of spillover can be corrected. In Fig. 3 the triple coincidences are divided into two mass ranges, one containing primarily O and the other primarily S, with only limited "cross contamination" that can be readily evaluated.

The striking difference between the solar wind and magnetospheric compositions (Fig. 2) was essentially due to the high abundance of Iogenic S and O ions in Jupiter's magnetosphere. Also, the charge state distributions of the two ion populations were totally different. Whereas the solar wind ions were nearly equilibrated in the ~10^6 K environment of the low corona

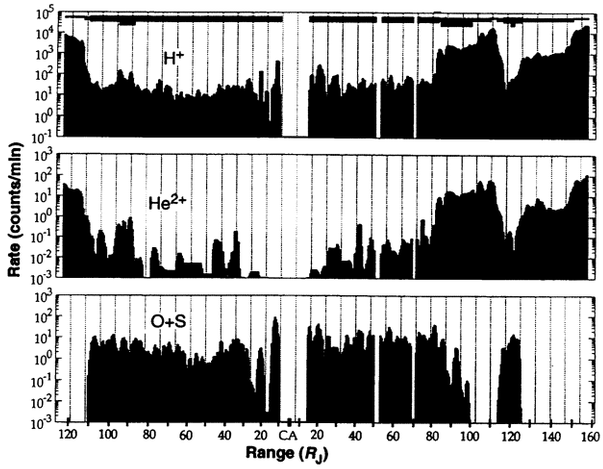

Fig. 1. Plot of the counting rates (10^5 count/min ~ 1 cm^{-3}) of 0.6 to 60 keV/charge H^+ (top panel), He^{2+} (middle panel), and the sum of O^+, O^{2+}, S^{2+}, S^{3+}, and S^{4+} (bottom panel) ions versus radial distance (1 R_J = 71,372 km) from Jupiter, measured in the Earth-pointing 120° field of view of SWICS. The horizontal bars at the top of the upper panel indicate the extent of interplanetary (thinnest bar), magnetosheath, magnetosphere, and mixed plasma (thickest bar) regions, respectively, near Jupiter; the dotted vertical lines in each panel are placed at 10-hour intervals starting at the beginning of day 33. The gap (10 ~ R_J inbound to ~ 14 R_J outbound) near closest approach (6.3 R_J) is due to the reduced sensitivity to which SWICS was configured in order to prevent damage of the microchannel plates from the intense penetrating electron fluxes. Low charge-state S and O ions from Io were observed throughout the entire magnetosphere as well as in the mixed plasma regions in the outer magnetosphere. While He^+ of solar wind origin penetrates deep into the magnetosphere, its flux was greatly reduced in the innermost region (≤30 R_J) investigated. For H^+ and the O + S ions, on the other hand, relatively high fluxes showing 10-hour periodicity were observed in the middle magnetosphere.

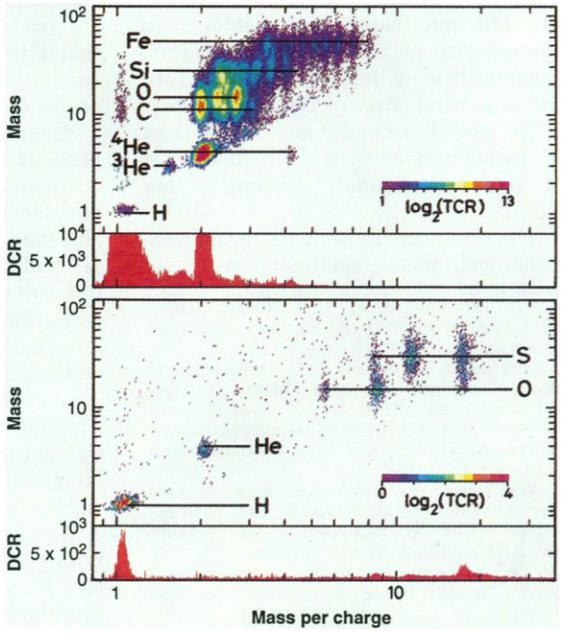

Fig. 2. Mass versus mass/charge matrix of solar wind (top) and Jupiter magnetosphere plasma (bottom). The triple coincidence rates (TCR) are color-coded in the upper part of the panels, while the double coincidence rates (DCR), for which no mass information was available, are given as histograms below. The Jupiter data are the sum over all periods IN1 through OUT4, and the solar wind data were collected well after the encounter on days 57 to 76, March 1992. The change in charge state and elemental composition is striking. Since raw counts are given, abundance ratios cannot be estimated from this figure.

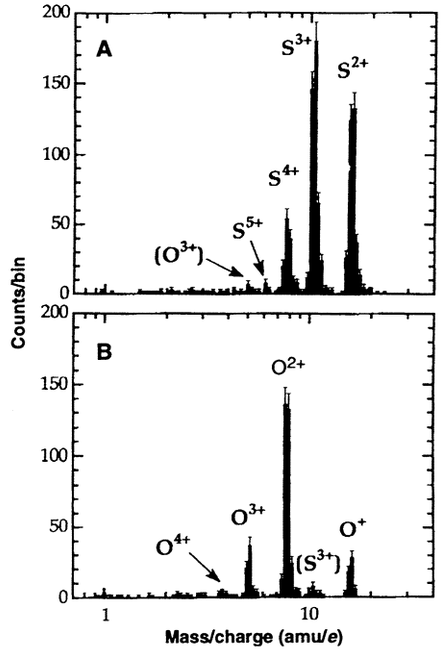

Fig. 3. Mass/charge spectra [in atomic mass units (amus) per electron charge (*e*)] of triple coincidence ions in Jupiter's magnetosphere. (**A**) Mass range 20 to 50 amus, showing mostly the S^{2+} to S^{5+} ions. In these spectra S^+ ions were very rare because they are quite inefficient in producing a triple coincidence. (**B**) Mass range 10 to 20 amus, showing mostly the four low-charge states of oxygen. Brackets indicate trace amounts of these ions.

(8), the average charges of the S and O ions in the magnetosphere remained far below the values that would have corresponded to an equilibrium with the ambient electron gas.

Three phase space density plots of H^+ appear in Fig. 4, each covering two adjacent regions defined in Table 1. From such plots, densities, temperatures, and other moments can be derived, and the possible presence of thermally different components of an ion species becomes apparent. The number densities and temperatures given are indicative only; they were calculated based on the assumption of isotropic and spatially uniform velocity distributions. For H^+ (as well as for other species) there are two or three thermally different components (Fig. 4). The energy coverage of SWICS was sufficient to investigate the "hot" (~10 keV) and "warm" (~1 keV) components of the plasma (Fig. 4). We expect improved density and temperature estimates and to investigate field-aligned ion streaming or corotation by analyzing the arrival directions of individual ion species.

The M/q spectra measured in the seven selected magnetospheric regions appear in Fig. 5. The $O^+ + S^{2+}$, S^{3+}, and O^{2+} ions produced the three dominant peaks in the M/q range. Undoubtedly their origin was Io, because S-O compounds are major components in the gases liberated from this satellite (*9*, *10*). Our data confirm the widespread and large abundance of Iogenic ions found by the Voyager Plasma Experiment (*11*). Whereas the Voyager cold plasma composition data inside and near the Io torus are unique, Ulysses-SWICS has provided us with new information on the composition of the hot plasma in the middle and outer magnetosphere. In all these regions, S and O ions of different charge states could be distinguished (see also Figs. 2 and 3), which will allow us to derive abundance ratios of these important ions throughout the magnetosphere. Moreover, by virtue of Ulysses' trajectory SWICS has

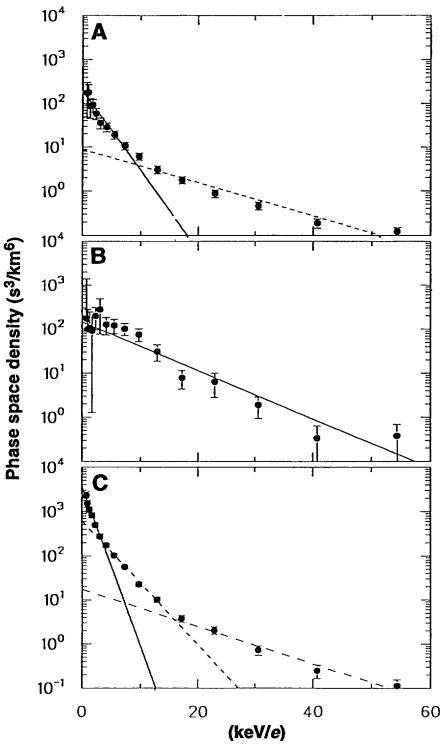

Fig. 4. Distribution functions of H^+ in three time intervals during the Jupiter encounter. We observed a multitemperature plasma composed of a hot component above $E/q \simeq 10$ keV with a temperature of $kT \simeq 10$ keV and a warm component at low E/q with a temperature of $kT \simeq 1$ to 3 keV. The hot component fills the entire magnetosphere traversed by Ulysses with a density of a few times 10^{-4} cm^{-3}, while the warm component is more variable: it was less abundant inbound than outbound and for H^+ was absent in the innermost magnetospheric regions investigated (OUT1 through OUT2). (**A**) IN2 through IN3: solid line, $kT = 2.4$ keV ($n = -0.00032$ cm^{-3}); dotted line, $kT = 11.5$ keV ($n = 0.00016$ cm^{-3}). (**B**) OUT1 through OUT2: solid line, $kT = 7.9$ keV ($n = 0.0015$ cm^{-3}). (**C**) OUT3 through OUT4: solid line, $kT = 1.2$ keV ($n = 0.0022$ cm^{-3}); dashed line, $kT = 10.3$ keV ($n = 0.00027$ cm^{-3}); dotted line, $kT = 3.1$ keV ($n = 0.0016$ cm^{-3}).

Fig. 5. The mass/charge spectra obtained in the seven selected regions (Table 1). Plotted are sums of the double and triple coincidence PHA counts corrected for the bias introduced by our priority scheme. These data must be corrected for background and efficiencies to derive abundance ratios. Iogenic ions dominated in the mass/charge range of 4 to 36 presented.

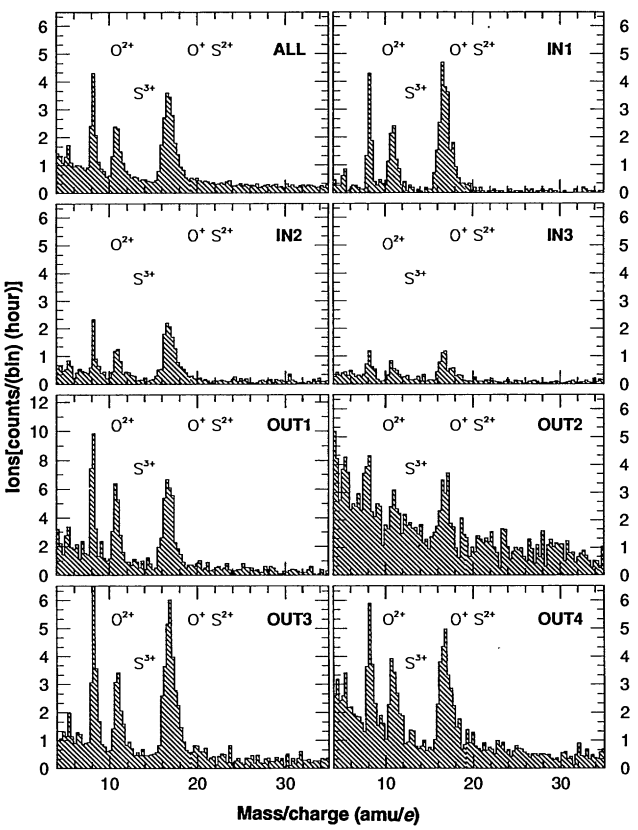

Table 1. Summary of time intervals for which data were analyzed; SCET, spacecraft event time.

Data interval	Time interval (SCET)	Distance to Jupiter (R_J)	B Field (*7*) (nT)	Angle between spin axis and B direction (°) (*7*)
IN1	033:23:00–034:14:00	108.9–97.8	0.8–5.8	45–150
IN2	035:04:00–036:15:00	87.2–60.5	0.4–8.7	15–150
IN3	036:15:00–038:13:00	60.5–23.3	0.9–60.0	15–135
OUT1	040:02:00–040:12:00	15.6–24.2	65.0–180.0	60–180
OUT2	040:12:00–041:00:00	24.2–34.2	30.0–65.0	40–60
OUT3	041:00:00–042:10:00	34.2–61.3	8.0–30.0	35–75
OUT4	042:10:00–043:12:00	61.3–81.2	6.2–14.0	40–75

Table 2. Ions of different sources in Jupiter's magnetosphere.

Solar wind	H^+, He^{2+}, O^{6+}
Jupiter	H^+, (H_2^+, H_3^+)*
Io	O^+, O^{2+}, O^{3+}, (O^{4+}), (Na^+, K^{2+}), S^+, S^{2+}, S^{3+}, S^{4+}, (S^{5+})
Icy satellites	(H_2O^+, H_3O^+)
Source undetermined	He^+

*Tentative identifications in parentheses (water group ions and K^{2+} are actually alternatives).

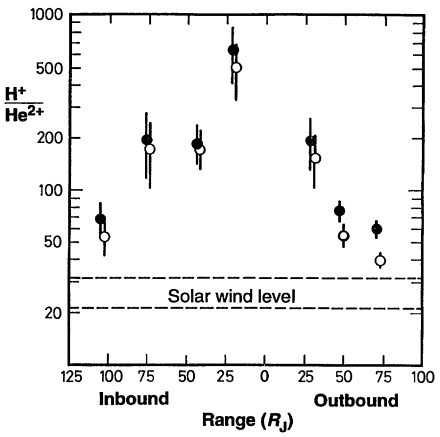

Fig. 6. Flux ratios of H^+/He^{2+} in the magnetospheric plasma derived from ions that were classified on board as Matrix Element and Matrix Rate events by SWICS. Double and triple coincidences were used for H^+, but for He^{2+} only triple coincidences were used, to give an unambiguous distinction from H_2^+. Because there are no energy spectra for the triple coincidence He^{2+} data, we give two limiting values for H^+/He^{2+}, assuming that the ions had either the same energy/charge (open circles) or the same energy/mass (filled circles) spectrum. Space between dashed lines, solar wind level. For the range, zero represents the point of closest approach.

provided us with the first composition data in the high-latitude regions on the dusk side (OUT1 to OUT4), and these data demonstrate the omnipresence of a strong Iogenic plasma component in the entire middle and outer magnetosphere at all latitudes (see also Fig. 1). Although we cannot report now on the relative abundance of S^+, there seem to be no striking systematic differences in the relative abundances of the major Iogenic ions $O^+ + S^{2+}$, S^{3+}, and O^{2+} along the entire magnetospheric path of Ulysses. Outside the torus region, large-scale mixing, loss from the magnetospheric reservoir, or both, seem faster than electron stripping (*12*).

Neutral Na and K clouds were observed in the Io torus (*13*), and Na ions were detected at medium (*14*) and high (*15*) energies in the magnetosphere. We have tentatively identified Na^+: its abundance was low, less than 5% relative to the sum of the O ions. There may be a trace of K^{2+}, but we cannot readily distinguish it from water group ions.

The He^{2+} ion is our best indicator for the presence of solar wind ions in the magnetospheric plasma. We do not expect a significant fraction of this ion to come from the Jovian ionosphere because the abundance of its progenitor, He^+, is kept relatively low there by reactions with H_2 (*15*). We found a finite abundance of He^{2+} in all seven magnetospheric regions (Figs. 1 and 6 and Table 1), indicating that there is a significant solar wind component in the plasma throughout the outer and middle magnetosphere.

Ions from Jupiter's ionosphere are not easy to distinguish from solar wind ions, because the sun and Jupiter have much the same chemical composition. The low-energy charged particle investigation on the Voyager spacecraft discovered H_2^+ and H_3^+ among the energetic particles (>200 keV per nucleon), hitherto the most direct demonstration of an ionospheric component in the Jovian magnetosphere (*17*). We have tentatively identified H_2^+ and H_3^+ in region OUT2 and we also found traces of He^+, some or most of which might have come from Jupiter (other possible contributions are He ions of interstellar origin or charge-exchanged solar wind α particles). However, we can best estimate the relative abundance of ionospheric material in the Jovian magnetosphere from H^+/He^{2+} observations. This method has been successfully applied in the magnetosphere of Earth, where detailed analyses of energy distributions showed that the H^+/He^{2+} ratio of the solar component in various magnetospheric regions is similar to the solar wind value (*18*). The H^+/He^{2+} flux ratios found in the Jovian magnetosphere are shown in Fig. 6. Although these data are preliminary and we hope to improve them, the variations shown in Fig. 6 are real. Whereas the H^+/He^{2+} ratios in the outer regions (IN1, OUT3, and OUT4) approached the normal solar wind values, they increased systematically with decreasing distance from Jupiter. In the OUT1 region H^+/He^{2+} was far above the range of typical solar wind values, which leads us to conclude that most of the H here stems from the Jovian ionosphere. It is likely that the H in regions IN2, IN3, and OUT2 contains a significant Jovian component as well. Because H^+ is the most abundant species in the solar wind and Jupiter's ionospheric plasma, our data imply that both are important as sources of the magnetospheric plasma, with the solar wind contributing more to the outer regions and Jupiter more to the inner regions.

Io may not be the only moon to supply ions to Jupiter's magnetosphere. Sputtering could liberate components of the icy material from Europa or other Galilean satellites (*19*). It has been suggested that water group ions are abundant in the Saturnian magnetosphere (*20*), but such ions have not been found in the Jovian magnetosphere. We have tentatively identified the water group ions H_2O^+, H_3O^+, or both: in many regions we observed a pronounced shoulder above the S^{2+}-O^+ peak (see also Fig. 5) at an M/q of about 18 to 19. The shoulder could be due to the water group ions, but we would not exclude a contribution from low-charged metals such as K^{2+} (*21*).

Ion species unambiguously identified so far are listed in Table 2. Material from three sources, the solar wind, the planet Jupiter, and the volcanic satellite Io, can be traced by source-specific ions. Significant amounts of solar wind and Iogenic particles were found in all regions we investigated, proving that solar wind plasma penetrates deep into the magnetosphere and that Iogenic ions advance to its outer reaches at both low and high latitudes. Jovian ions were more abundant than solar wind ions in the inner regions and less abundant in the outer regions. These findings place constraints on models of plasma circulation, radial transport, and loss from the magnetosphere. The Iogenic ions dominate the mass density, and consequently the average ionic mass is high in all investigated regions at low and high latitudes. This identification of ion masses is needed for proper assessment of the centrifugal and pressure terms in the stress balance equation [see also (*2*)].

REFERENCES AND NOTES

1. T. W. Hill, A. J. Dessler, C. K. Goertz, in *Physics of the Jovian Magnetosphere*, A. J. Dessler, Ed. (Cambridge Planetary Science Series, Cambridge Univ. Press, Cambridge, 1983), p. 353.
2. V. M. Vasyliunas, in *ibid.*, p. 395.
3. G. Gloeckler *et al.*, *Astron. Astrophys. Suppl. Ser.* **92**, 267 (1992).
4. The SWICS data are received in three forms: A small sample of directly transmitted pulse height (PHA) events (with detailed information on mass, charge, E/q, and angles of incidence); the Matrix Element counts (only mass and charge information integrated over all energies; classification on the spacecraft); and the Matrix Rates (information with decreased resolution on mass, charge, and E/q; classification on the spacecraft).
5. The background was very low for the triple coincidence rates but was appreciable for the double coincidences, especially inside ~35 R_J. Because the solid-state detectors of the main channel of SWICS have thresholds of about 40 keV, we depend largely on double coincidences for low-charged ions, requiring background subtraction.
6. The O + S count rates are systematically lower inbound than outbound. This is due to the orientation of the entry system, which did not accept corotating ions on the inbound pass. On the outbound pass, acceptance of corotating ion populations increased with R_J, so the O + S density may not have been as constant as the count rates in Fig. 1. Still, it is remarkable that high abundances of O and S ions are observed far from the plasma sheet.
7. A. Balogh *et al.*, *Science* **257**, 1515 (1992).
8. A. Bürgi and J. Geiss, *Sol. Phys.* **103**, 347 (1986).
9. S. Kumar and L. Pearl, *Am. Astron. Soc. Bull.* **11**, 593 (1979).
10. F. M. Neubauer, *ibid.*, p. 592.
11. H. S. Bridge *et al.*, *Science* **204**, 987 (1979); H. S. Bridge *et al.*, *ibid.* **206**, 972 (1979); R. L. Mc Nutt, J. W. Belcher, H. S. Bridge, *J. Geophys. Res.* **86**, 8319 (1981); J. W. Belcher, in (*1*), p. 68; F. Bagenal, D. E. Shemansky, R. L. McNutt, Jr., R. Schreier, A. Eviatar, *Geophys. Res. Lett.* **19**, 79 (1992).
12. The relatively modest but significant differences in the charge-state distributions of O and S, apparent even in the count-rate spectra of Fig. 5, will be further explored in a later publication.
13. L. Trafton, *Rev. Geophys. Space Phys.* **19** (no. 1), 43 (1981).

14. S. M. Krimigis, J. F. Carbary, E. P. Keath, C. O. Bostrom, W. I. Axford, *J. Geophys. Res.* **86**, 8827 (1981); S. M. Krimigis and E. C. Roelof, in (*1*), p. 106.
15. R. E. Vogt *et al.*, *Science* **206**, 984 (1979).
16. D. F. Strobel and S. K. Atreya, in (*1*), p. 51.
17. D. C. Hamilton *et al.*, *Geophys. Res. Lett.* **7**, 813 (1980).
18. H. Balsiger, in *High-Latitude Space Plasma Physics*, B. Hultqvist and T. Hagfors, Eds. (Plenum, New York, 1983), p. 313.
19. L. J. Lanzerotti *et al.*, *Geophys. Res. Lett.* **5**, 155 (1978).
20. R. E. Johnson *et al.*, *Icarus* **77**, 311 (1989); E. Eviatar and J. D. Richardson, *Ann. Geophys.* **8**, 725 (1990).
21. An unambiguous identification is not easy in this case because these are double coincidence counts that have a relatively high background and because the position of molecular ions on the *M/q* scale is not exactly the same as for atomic ions. By studying these events specifically, we may be able to confirm the existence of water group ions, which would most likely come from the icy satellites.
22. We thank P. Bedini, S. Lasley, F. Ottens, W. Rieck, C. Shafer, and R. Wimmer for supporting the SWICS experiment during the Ulysses-Jupiter Encounter, and the Ulysses teams of the European Space Agency–European Space Operations Center/European Space Technology Center and the National Aeronautics and Space Administration–Jet Propulsion Laboratory for their excellent work during this crucial period. Supported by the Swiss National Science Foundation, NASA contract JPL 955460, and the Bundesminister für Forschung und Technologie of Germany.

29 May 1992; accepted 28 July 1992

Jupiter's Magnetosphere: Plasma Description from the Ulysses Flyby

Samuel J. Bame,* Bruce L. Barraclough, William C. Feldman, Galen R. Gisler, John T. Gosling, David J. McComas, John L. Phillips, Michelle F. Thomsen, Bruce E. Goldstein, Marcia Neugebauer

Plasma observations at Jupiter show that the outer regions of the Jovian magnetosphere are remarkably similar to those of Earth. Bow-shock precursor electrons and ions were detected in the upstream solar wind, as at Earth. Plasma changes across the bow shock and properties of the magnetosheath electrons were much like those at Earth, indicating that similar processes are operating. A boundary layer populated by a varying mixture of solar wind and magnetospheric plasmas was found inside the magnetopause, again as at Earth. In the middle magnetosphere, large electron density excursions were detected with a 10-hour periodicity as planetary rotation carried the tilted plasma sheet past Ulysses. Deep in the magnetosphere, Ulysses crossed a region, tentatively described as magnetically connected to the Jovian polar cap on one end and to the interplanetary magnetic field on the other. In the inner magnetosphere and Io torus, where corotation plays a dominant role, measurements could not be made because of extreme background rates from penetrating radiation belt particles.

During the Ulysses flyby of Jupiter, analogs of the familiar plasma regions and boundaries found in Earth's magnetospheric system were observed, including upstream electron and ion precursors of the bow shock, bow shock, magnetosheath, magnetopause and its boundary layer, outer and middle magnetosphere, and plasma sheet. With the exceptions of the larger scale of the Jovian system, its higher rotation rate, and the presence of the Io torus, the similarities between features in the magnetosphere of the Jovian system and of the terrestrial system are striking. Finding these similarities reinforces the idea that these features are common astrophysical phenomena that can be expected in other similar systems that may be inaccessible to space probes. These observations supplement and extend those of the earlier Pioneer (*1*) and Voyager (*2*) flyby missions because Ulysses flew during a different time era, along a different encounter trajectory (*3*), and carried instrumentation having different capabilities. Here, we report an overview of the observations made with the Ulysses solar wind plasma experiment.

Because the velocity distributions of ions and electrons in the solar wind are very different, the experiment contains two spectrometers (*4*) to characterize them independently in three dimensions: one for the beam-like ions and one for the omnidirectional electrons. Detailed descriptions of the instruments are given elsewhere (*5*). Even though not ideally suited for magnetospheric observations, the instruments measured many of the plasma features of the Jovian magnetosphere during the entire 15-day flyby except for the day of closest approach. The electron results are displayed in a color-coded spectrogram of energy distributions in Fig. 1; Fig. 2, A and B, presents a plot of electron density and temperature parameters with various features of the encounter identified. The summary chart in Fig. 3 shows the flight path of Ulysses with magnetospheric features located along the trajectory. Spectrograms for both electrons and ions from two intervals on the outbound leg are shown with time expanded in Figs. 4 and 5. A summary log of the entry and exit times of the various plasma regions is presented in Table 1 with boundary identifications. More precise boundary locations will be determined later from a joint analysis of plasma and field (*6*) observations.

At 17:33 UT (universal time) on day 33 (2 February 1992), an abrupt appearance in the Fig. 1 spectrogram of a broad band of yellow extending to energies above 100 eV marks a single inbound crossing of the bow shock, where the solar wind electrons were heated and compressed. An ion spectrogram (not presented here) shows that the solar wind proton and helium ions were similarly heated, compressed, and deflected. A model consistent with past flyby results predicts a bow shock at ~80 Jupiter radii (R_J) for average solar wind conditions. Instead, this crossing, located in Fig. 3, occurred at 113 R_J as the magnetosphere expanded in response to a measured factor of 10 decrease of solar wind dynamic pressure during the day before the crossing. Quantitative electron density and temperature (T) jumps at the shock are ~0.06 to ~0.15 electron cm^{-3} and ~1.6×10^5 to ~1.3×10^6 K, respectively. The amount of heating at this crossing and other crossings during the flyby shows that ΔT scales as the change in flow velocity (ΔV) in the same manner as at Earth. This fact, combined with the fact that the downstream electron distributions had the flattened tops characteristic of distributions downstream from Earth's bow shock, suggests a heating mechanism at Jupiter like that at Earth. Figure 3 also locates several upstream episodes of interplanetary magnetic field (IMF) connection to the bow shock, observed at Jupiter for the first time in three-dimensional distributions of the solar wind electron velocity. Connection events have been observed many times at Earth (*7*) and also at comet Giacobini-Zinner (*8*). When connected, a flux of hot electrons from the shock streams sunward along the IMF, counterflowing against the usual electron heat flux from the hot solar corona.

From previous flybys it was expected that nearly a day would be required for Ulysses to cross the magnetosheath into the magnetosphere. Instead, this crossing, identified in the spectrogram in Fig. 1 by the

S. J. Bame, B. L. Barraclough, W. C. Feldman, G. R. Gisler, J. T. Gosling, D. J. McComas, J. L. Phillips, M. F. Thomsen, Space Plasma Physics Group, MS D438, Los Alamos National Laboratory, Los Alamos, NM 87545.
B. E. Goldstein and M. Neugebauer, Mail Stop 169-506, Jet Propulsion Laboratory, California Institute of Technology, 4800 Oak Grove Drive, Pasadena, CA 91109.